Phenotypic Characterization of an α_4 Neuronal Nicotinic Acetylcholine Receptor Subunit Knock-Out Mouse

Shelley A. Ross,[1] John Y. F. Wong,[1] Jeremiah J. Clifford,[3] Anthony Kinsella,[4] Jim S. Massalas,[1] Malcolm K. Horne,[1] Ingrid E. Scheffer,[1,5] Ismail Kola,[2] John L. Waddington,[3] Samuel F. Berkovic,[5] and John Drago[1]

[1]*Neurosciences Group, Monash University Department of Medicine and* [2]*Institute of Reproduction and Development, Monash Medical Centre, Clayton, Victoria, 3168, Australia,* [3]*Department of Clinical Pharmacology, Royal College of Surgeons in Ireland, Dublin 2, Ireland,* [4]*Department of Mathematics, Dublin Institute of Technology, Dublin 8, Ireland, and* [5]*Department of Medicine, University of Melbourne, Austin and Repatriation Medical Centre, Heidelberg, Victoria, 3084, Australia*

Neuronal nicotinic acetylcholine receptors (nAChR) are present in high abundance in the nervous system (Decker et al., 1995). There are a large number of subunits expressed in the brain that combine to form multimeric functional receptors. We have generated an α_4 nAChR subunit knock-out line and focus on defining the behavioral role of this receptor subunit. Homozygous mutant mice (Mt) are normal in size, fertility, and home-cage behavior. Spontaneous unconditioned motor behavior revealed an ethogram characterized by significant increases in several topographies of exploratory behavior in Mt relative to wild-type mice (Wt) over the course of habituation to a novel environment. Furthermore, the behavior of Mt in the elevated plus-maze assay was consistent with increased basal levels of anxiety. In response to nicotine, Wt exhibited early reductions in a number of behavioral topographies, under both unhabituated and habituated conditions; conversely, heightened levels of behavioral topographies in Mt were reduced by nicotine in the late phase of the unhabituated condition. Ligand autoradiography confirmed the lack of high-affinity binding to radiolabeled nicotine, cytisine, and epibatidine in the thalamus, cortex, and caudate putamen, although binding to a number of discrete nuclei remained. The study confirms the pivotal role played by the α_4 nAChR subunit in the modulation of a number of constituents of the normal mouse ethogram and in anxiety as assessed using the plus-maze. Furthermore, the response of Mt to nicotine administration suggests that persistent nicotine binding sites in the habenulo-interpeduncular system are sufficient to modulate motor activity in actively exploring mice.

Key words: α_4; nicotinic receptor; homologous recombination; anxiety; knock-out; behavioral topography

Nicotine is one of the most widely consumed psychoactive drugs and exerts a number of pharmacological actions in the CNS and PNS (Decker et al., 1995). Neuronal nicotinic acetylcholine receptors (nAChR) constitute a heterogenous family of pentameric oligomers with contributions from 11 subunits (Le Novere and Changeux, 1995). Five types of α subunits (α_2–α_6) and three types of β subunits (β_2–β_4) permit combinations of α and β type subunits to form a number of functional receptors with subunits of two or more different types (Changeux et al., 1998), whereas subunits α_7–α_9 can form α-bungarotoxin-sensitive homopentameric receptors (Corringer et al., 1995). The topography of nAChR subunits varies (Deneris et al., 1989; Duvoisin et al., 1989; Wada et al., 1989, 1990; Hill et al., 1993; Elgoyhen et al., 1994; Court and Perry, 1995; Le Novere et al., 1996; Brioni et al., 1997; Zoli et al., 1998), with α_4 and β_2 transcripts being found in a large number of CNS nuclei, whereas α_2, α_3, α_5, α_6, β_3, and β_4 mRNAs are restricted to a few cholinergic pathways, which also express α_5 and β_2.

Despite detailed characterization of nAChR subunits at the molecular level, not much is known about the *in vivo* functional role of individual subunits. Most nAChR ligands show similar patterns of high-affinity labeling that resembles the distribution of α_4/β_2 subunits. A number of nAChR agonists that bind to the α_4/β_2 receptor configuration *in vitro* are known to have an effect on anxiety (Pomerleau, 1986; Gilbert et al., 1989; Brioni et al., 1993), attention (Brioni et al., 1997), and antinociception (Tripathi et al., 1982; Damaj et al., 1998), implicating the α_4/β_2 receptor in the mediation of a number of physiological processes. Analysis of an independently generated line of α_4 nAChR subunit knock-out mice (Marubio et al., 1999) validated the significant role played by this receptor subunit in nociception. Loss of nicotinic binding sites and a decrease of nAChR protein expression has been shown in patients with Alzheimer's disease and patients with Parkinson's disease with cognitive dysfunction (Giacobini, 1991; Brioni et al., 1997). Furthermore, several mutations in the α_4 nAChR subunit have been identified in autosomal dominant nocturnal frontal lobe epilepsy (Steinlein et al., 1995, 1997). The large number of subunits suggests a potential for considerable diversity in nAChR function(s). Defining the specific role played by individual subunits in determining spontaneous motor behavior and responses to drug challenge will be aided by ongoing analysis of nAChR subunit gene knock-out mice (Picciotto et al., 1995; Orr-Urtreger et al., 1997; Marubio et al., 1999; Xu et al., 1999).

Nicotine is known to reduce anxiety in both chronic smokers (Gilbert, 1979; Pomerleau, 1986; Gilbert et al., 1989) and nonsmokers (Hutchinson and Emley, 1973). Anxiolytic-like effects of nicotine and a select number of neuronal nicotinic receptor agonists have also been documented in experimental animals (Costall et al., 1989; Brioni et al., 1993; Cao et al., 1993). The differential behavioral profile of neuronal nicotinic agonists implies that the anxio-

Received Jan. 10, 2000; revised June 9, 2000; accepted June 14, 2000.

This work is supported in part by the National Health and Medical Research Council of Australia (NHMRC), the Australian Commonwealth Department of Veteran's Affairs, and an unrestricted educational grant from Parke-Davis (Australia). S.R. was supported by a Peter Bladin Scholarship from the Epilepsy Society of Australia. J.D. is a Monash University Logan Research Fellow. J.J.C. was supported by the NHMRC Brain Network into Mental Health Diseases. J.L.W. and J.J.C. are supported by a Galen Fellowship from the Irish Brain Research Foundation. the Higher Education Authority of Ireland. and the Royal College of Surgeons in Ireland. We thank Prof. Bevyn Jarrott (Department of Pharmacology, Monash University) for the gift of iodinated α-bungarotoxin. We also thank Dr. Ian Simpson for his help with organ histology.

J.Y.F.W. and J.J.C. contributed equally to this work.

Correspondence should be addressed to Dr. J. Drago, Department of Medicine, 5th Floor E Block, Monash Medical Centre, Clayton Road, Clayton, Victoria, 3168, Australia. E-mail: john.drago@med.monash.edu.au.

 0270-6474/00/206431-11$15.00/0

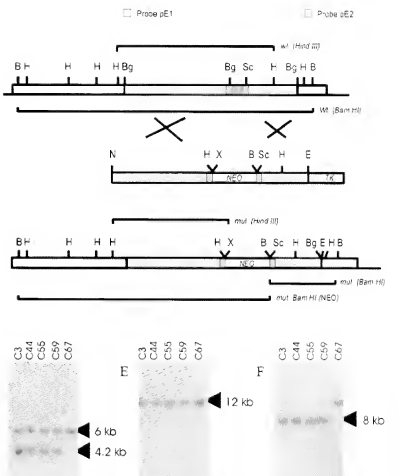

Figure 1. Construction of targeting vector and Southern blot analysis of ES clones. Representation of the genomic map of the α_4 nAChR gene (*A*), the targeting vector (*B*), and the expected allelic disruption after homologous recombination (*C*). The restriction sites shown are abbreviated as follows: *N*, *Not*I; *H*, *Hin*dIII; *Bg*, *Bgl*II; *Sc*, *Sca*I; *X*, *Xho*I; *E*, *Eco*RI; *B*, *Bam*HI. *NEO* represents the neomycin phosphotransferase resistance gene, and *TK* represents the thymidine kinase gene. The origin of the probes used for homologous recombination screening are also shown. Probe pE1 is a *Hin*dIII-*Bgl*II fragment used to confirm 5′ recombination, and probe pE2 is a *Hin*dIII-*Bam*HI fragment used for confirmation of 3′ recombination. *D* shows the Southern blot of *Hin*dIII-digested ES cell genomic DNA probed with pE1 (Wt allele is 6 kb, and the recombinant allele is 4.2 kb), showing correctly targeted clones (C3, C44, C55, and C59); C67 is a randomly selected nontargeted clone. *E* shows the Southern blot of *Bam*HI-digested ES cell genomic DNA probed with pE2; the Wt allele is 12 kb, and the recombinant allele is 2.5 kb (clones C3, C44, C55, and C59 are correctly targeted). *F* shows a Southern blot of a *Bam*HI-digested probed with a NEO-specific probe. Clones C3, C44, C55, and C59 have a single band at the expected size of 8 kb, confirming a single insertion event in all the clones examined.

lytic actions of nicotine may be mediated by a specific subunit configuration of the nAChR. We generated an α_4 nAChR knock-out line to test the hypothesis that mice lacking α_4 nAChR subunits would show behavioral features consistent with heightened basal levels of anxiety.

MATERIALS AND METHODS

Animals. All procedures involving the use of live animals conformed to the National Health and Medical Research Council (NHMRC) code of practice.

Cloning. A 1.0 kb cDNA probe encoding the putative second transmembrane domain of the α_4 nAChR receptor subunit was cloned by PCR amplification of embryonic stem (ES) cell-derived genomic DNA using primers based on conserved regions between the human (GenBank accession number 135901) and rat (GenBank accession number 131620) published cDNA sequence. The forward primer corresponded to nucleotides 484–509, and the reverse primer corresponded to nucleotides 1472–1500 of the rat sequence. An 11.2 kb clone was isolated, and homologous flanks were cloned into the pPNT targeting vector (Tybulewicz et al., 1991). The construct was designed to create a nonfunctioning allele by removing a 750 bp *Bgl*II/*Sca*I fragment from the fifth exon (Fig. 1). This fragment contains DNA spanning from the first hydrophobic transmembrane domain through to the second intracytoplasmic loop. The 5′ flank was a 4.0 kb *Bgl*II fragment, and the 3′ flank was a 2.0 kb *Sca*I/*Bgl*II fragment (Fig. 1).

ES cell culture and molecular analysis of transgenic mice. Linearized targeting construct (50 μg) was electroplated into the J1 line (a gift from Dr. R. Jaenisch, Massachusetts Institute of Technology, Cambridge, MA) of ES cells using standard techniques (Drago et al., 1994). A *Hin*dIII digest of ES cell clone-derived genomic DNA probed with pE1 (Fig. 1) was used to verify recombination at the 5′ end (normal allele is 6.0 kb and the recombinant allele 4.2 kb). A Southern blot of a *Bam*HI digest probed with pE2 was used to verify 3′ recombination (normal allele is 12.0 kb and recombinant allele is 2.5 kb). A single incorporation event was confirmed by probing a *Bam*HI Southern blot with a neomycin phosphotransferase (NEO) gene cDNA probe (Fig. 1). Four recombinants were identified by Southern blotting (Fig. 1), one of which (C3) was injected into BALB/C blastocysts, and chimeras were generated. Chimeras were mated with CF1 mice, and a single heterozygous mouse (Hz) was obtained. The Hz founder was used to generate the entire colony by subsequent crossing with C57/BL6 mice. Hz progeny, obtained after two backcrosses with C57/BL6 mice, were mated to establish a number of muiant mice (Mt) mating pairs and wild-type mice (Wt) mating pairs. All Mt mice used in this study were therefore derived from Mt intermatings, and all Wt mice were derived from Wt intermatings. Maximal diversity in the genetic background was maintained by randomly interchanging breeders within a given genotype.

Tissue preparation. Adult (Wt, $n = 9$; Hz, $n = 9$; and Mt, $n = 11$) mice were killed by decapitation, and the brains were snap-frozen in cold isopentane and stored at −70°C before use. Twenty micrometer frozen coronal sections were cut in a cryostat and mounted onto 3-aminopropyl triethoxysilane (Sigma, St. Louis, MO) -coated slides for *in situ* hybridization and gelatin-coated slides for ligand binding studies.

In situ *hybridization. In situ* hybridization was performed for α_3, α_4, α_6, α_7, β_2, β_3, and β_4 nAChR subunits. The sequences of the oligonucleotides used are as shown in Table 1. Four oligonucleotides were designed to identify α_4 nAChR-specific transcript. Probes ISACh3 and ISACh4 were designed to hybridize with mRNA encoded in transcribed gene sequence upstream of the deleted *Bgl*II/*Sca*I fragment (Fig. 1), ISACh1 and ISACh2 were designed to hybridize with mRNA derived from this deleted sequence. This strategy allowed identification of cells that normally express the α_4 nAChR subunit in both Wt and Mt. as well as verified the knock-out paradigm. All oligonucleotide probes were 5′ end-labeled using a standard kinase protocol (Wong et al., 1997) with [γ-^{33}P]ATP and T4 polynucleotide kinase. Specificity of probes used in this study was determined by using a 100-fold excess of unlabeled antisense oligonucleotides added to the *in situ* hybridization reactions to competitively inhibit probe hybridization. Slides were exposed to Hyperfilm (Amersham Pharmacia Biotech, Uppsala, Sweden), and the images were scanned. The density of mRNA

Table 1. Antisense oligonucleotide probes

Nicotinic receptor subunit target	Probe code	Accession number	Probe position	Sequence of oligonucleotide	% GC
$\alpha 3$	$\alpha 3$	L31621	1038	CCCAAGTGGGCATGGTGTGTGTGGTTGGAGTTCTATAGTGCACAT	51
$\alpha 6$	$\alpha 6$#1	L08277	325	TCAAAGTGCACCGTGACGGGATCAGAAACGTTTTCCACTGGCCGG	55
$\alpha 6$	$\alpha 6$#2	L08277	1575	GCCCCACAGTTCCAAACACAGACGATTATAAACACCCAGAGGA	48
$\alpha 7$	$\alpha 7$	L37663	197	TCCATGATCTGCAGGAGGCTCAGGGAGAAGTACACGGTGAGCGGC	60
$\beta 2$	$\beta 2$#1	L31622	1455	TCGCATGTGGTCCGCAATGAAGCGTACGCCATCCACTGCTTCCCG	60
$\beta 2$	$\beta 2$#2	L31622	1341	AGCCAAGCCCTGCACTGATGCAGGGTTGACAAAGCAGGTACATGG	55
$\beta 3$	$\beta 3$#1	J04636	1315	CAGAACTCTTTCTCCATCGCTGGCGGGAGTCTGTTTCCTTTTGCC	53
$\beta 3$	$\beta 3$#2	J04636	440	ATTCTTCCGGATTCCAGCGTAATTTTTGGTCTGTCCATTCCTGCT	44
$\beta 4$	$\beta 4$#1	U42976	1322	AGCTGACACCCTCTAATGCTTCCTGTAGATCTTCCGGAACCTCC	53
$\alpha 4$	ISACh1			CGAGGTCGGGATGATCTCGGTGATGAGCAGCAGGAAGACGGTGAGAG	60
$\alpha 4$	ISACh2			TGGAGAGGGTGACGAAGATCAGGTGAAGAGCAGGTACTCGCCGATGAGCG	58
$\alpha 4$	ISACh3			GCTGTGCATGCTCACCAAGTCAATCTTGGCCTTGTCGTAGGTCCAGGACC	56
$\alpha 4$	ISACh4			CATAATGACCCACTCCCCACTTTCCCAGAAGTCCAGTTGGTCCACACGGC	56

All 45-mer oligonucleotide probes were based on published rat sequence, except for the $\alpha 7$ subunit, which is based on mouse sequence.
Accession numbers are from GenBank. G and C represent guanine and cytosine, respectively.

expression for α_4 ((ISACh3/4), α_5, α_4, α_6, α_7, β_2, β_4, and β_3 nAChR subunits was quantified using a microcomputer imaging device (MCID) with software (Image Research Inc., Brock University, St. Catherine's, Ontario, Canada). All values are expressed as counts per minute/square millimeter for mRNA expression (mean ± SEM). The specific binding for densitometric purposes was calculated by subtracting background binding (determined by cold competition) from results using labeled antisense oligonucleotides alone.

Receptor autoradiography. All nicotinic agonists were obtained from Sigma.

[^{3}H]nicotine binding. The slides were preincubated in Krebs'–Ringer's HEPES (in mM: NaCl 118, KCl 4.8, $CaCl_2$ 2.5, $MgSO_4 7H_2O$ 1.3, and HEPES 20, pH to 7.5 with NaOH) for 30 min at 4°C. They were then transferred to Krebs'–Ringer's HEPES containing 5.1 nM L-[*N*-methyl-^{3}H]nicotine (specific activity, 81.5 Ci/mmol; NEN, Boston, MA) and incubated for 90 min at 4°C. After incubation, the slides were washed as follows: two times for 5 sec each in Kreb's–Ringer's HEPES; two times for 5 sec each in 20 mM HEPES, pH 7.5; and two times for 5 sec each in distilled water. All washes were performed at 4°C. The slides were then air dried at room temperature and apposed to Hyperfilm (Amersham Pharmacia Biotech, Little Chalfont, UK) for 6 weeks in the presence of tritiated microscales (Amersham Pharmacia Biotech, Little Chalfont, UK). Binding in the presence of 1 μM unlabeled nicotine did not exceed film background.

[^{3}H]epibatidine binding. Slides were preincubated in Krebs'–Ringer's HEPES for 20 min at room temperature and then transferred to Krebs'–Ringer's HEPES containing 400 pM (±)[5,6-bicycloheptyl-^{3}H]epibatidine (33.8 Ci/mmol; NEN) for 60 min at room temperature. The slides were then washed as follows: two times for 10 sec each in Krebs'–Ringer's HEPES; two times for 10 sec each in 0.1× Krebs'–Ringer's HEPES; 10 sec in 5 mM HEPES, pH 7.5, and distilled water for 5 sec. All washes were performed at 0°C. The slides were then air dried at room temperature and apposed to Hyperfilm for 3 weeks together with standard tritiated microscales. Nonspecific binding was defined as the binding in the presence of unlabeled epibatidine (10 μM). Cold competition assays were also performed with unlabeled 300 μM nicotine and 150 nM cytisine.

[^{3}H]cytisine binding. The slides were incubated at 4°C for 60 min in 50 mM Tris-HCl, pH 7.4, containing (in mM): 120 NaCl, 5 KCl, 2.5 $CaCl_2$, 1 $MgCl_2$, and 5 [3,5-^{3}H (*N*)]cytisine hydrochloride (32Ci/mmol; NEN). The washes were as follows: three times for 2.5 min each in 50 mM Tris-HCl, pH 7.4, followed by a brief rinse in distilled water, all performed at 4°C. Nonspecific binding was defined as the binding in the presence of unlabeled nicotine (10 μM). The film was exposed for 3 months.

[^{125}I]α-bungarotoxin binding. The slides were preincubated in 50 mM Tris-HCl, pH 7.4, containing 0.1% bovine serum albumin (BSA) for 30 min at room temperature. They were then incubated in 50 mM Tris-HCl, pH 7.4, containing [^{125}I]α-bungarotoxin (2000 Ci/mmol; a gift from Prof. Bevyn Jarrott, Department of Pharmacology, Monash University, Clayton, Australia) at a concentration of 1.5 nM for 120 min at room temperature. The washes were as follows: two times for 15 min each in 50 mM Tris-HCl, pH 7.4, and 0.1% BSA; two times for 15 min each in 50 mM Tris-HCl, pH 7.4, followed by a brief rinse in distilled water, all performed at 4°C. Nonspecific binding was defined as the binding in the presence of unlabeled acetylcholine (10 mM). The slides were exposed to XAR5 film (Eastman Kodak, Rochester, NY) together with laboratory-prepared standards for 36 hr.

Binding densities were measured using the MCID M4 system under constant illumination. Standardization was achieved by comparing binding densities with ^{3}H-microscales and standards exposed with each film. All values are expressed as femtomoles per milligram of tissue for receptor binding studies (mean ± SEM). The specific binding was calculated by subtracting nonspecific binding determined when labeled ligand was coincubated with respective unlabeled receptor agonist.

Topography of spontaneous motor behavior. On experimental days, mice were removed from their home cage and placed individually in clear glass observation cages (36 × 20 × 20 cm). Behavioral assessments were performed in a manner similar to that used extensively for rats (Clifford and Waddington, 1998) and mice (Clifford et al., 1998, 1999) using a rapid time-sampling behavioral checklist technique. For this procedure, each of 10 randomly allocated mice was observed individually for 5 sec periods at 1 min intervals over 15 consecutive minutes, using an extended, ethologically based behavioral checklist. This allowed the presence or absence of the following individual behaviors (occurring alone or in any combination) to be determined in each 5 sec period: sniffing; locomotion (coordinated movement of all four limbs producing a change in location); total rearing (rearing of any form); rearing from a sitting position (front paws reaching upwards with hind limbs on floor in sitting position); rearing free (front paws reaching upwards away from any cage wall while standing on hind limbs); rearing toward a cage wall (front paws reaching upwards on a cage wall while standing on hind limbs); biting; sifting (sifting movements of the front paws through cage bedding material); grooming (of any form); intense grooming (grooming of the face with the forepaws followed by vigorous grooming of the hind flank or anogenital region with the snout); vacuous chewing (chewing movements not directed onto any physical material); chewing (chewing movements directed onto cage bedding and/or faecal pellets without consumption); eating (chewing with consumption); climbing (jumping onto cage top with climbing along grill in inverted or hanging position); and stillness (motionless, with no behavior evident). This cycle of assessment by behavioral checklist over a 15 min period (0–15 min) was repeated twice (20–35 and 40–55 min); therefore, 10 cycles of otherwise identical assessments were repeated at 80–90, 120–130, 160–170, 200–210, 240–250, 280–290, 340–350, and 360–370 min.

Effect of nicotine on behavior. Examination of the effect of nicotine was conducted under two conditions: (1) unhabituated, i.e., active exploration; and (2) habituated, whereby mice were placed individually in the clear glass observation cages and left undisturbed for a period of 3 hr. After injection of drug or vehicle, animals were assessed using the rapid time-sampling behavioral checklist technique. The time of injection was taken as the zero time point. For assessment of spontaneous behavior and effects of nicotine on unhabituated behavior, animals were used on one occasion only; for the assessment of effects of nicotine on habituated behavior, animals were used on two occasions, only separated by a drug-free interval of 1 week.

Rotarod. The rotarod apparatus (Ugo Basile, Milan, Italy) was used in accelerating mode, gradually increasing from 4 to 40 rpm over the course of 5 min. Mice were placed on the apparatus at a fixed speed of 4 rpm for 1 revolution; the apparatus was then set to accelerating mode, and the stopwatch was started. Latency to fall was recorded for each mouse in three trials per day, separated by an intertrial interval of 2 hr. Each mouse was subjected to this schedule for 3 successive days. Mice that stayed on the rotarod for >360 sec were considered complete responders; their latencies were recorded as 360 sec. All experiments were performed during the hours of 11:00 A.M. to 6:00 P.M. to avoid circadian effects.

Elevated plus-maze. Anxiolytic-like activity was evaluated using the elevated plus-maze, a pharmacologically validated model (Pellow et al.,

1985; Brioni et al., 1993), according to procedures described previously in which nicotinic receptor agonists were demonstrated to have an anxiolytic-like effect (Brioni et al., 1993). The elevated plus-maze was custom-made of black Perspex consisting of two open arms (5 × 30 cm) and two enclosed arms (5 × 30 × 14 cm) extending from a central platform (5 × 5 cm) mounted on a wooden base raised 57 cm above the floor; thus, the maze formed a "plus" shape. Overhead light levels on the open and enclosed arms were similar. At the beginning of the experiment, mice were placed in the center of the maze facing an enclosed arm, and the following variables were scored: (1) the time spent on the open and enclosed arms, reported as time spent on open (or enclosed) arms expressed as a percentage of total time (300 sec); and (2) the number of entries into open and closed arms. An arm entry was defined as the entry of all four feet of the animal into one arm; an arm exit was defined by the exit of both forelimbs from one arm. Plus-maze behavior was assessed by direct observation.

Data analysis. For determination of ethograms for spontaneous behavior over the phase of initial exploratory activity, the total "counts" for each individual behavior was determined as the number of 5 sec observation windows in which a given behavior was evident, summed over the initial 3 × 15 min (0–15, 20–35, and 40–55 min) cycle periods and expressed as means ± SEM. Data for individual behaviors were analyzed using ANOVA following square-root transformation, to allow examination of interaction effects in the absence of nonparametric techniques for interaction terms. For determination of the habituation profiles of these ethograms, total counts for each individual behavior were summed as above over each of the following periods: 0–10, 20–30, 40–50, 80–90, 120–130, 160–170, 200–210, 240–250, 280–290, 340–350, and 360–370; these were expressed also as means ± SEM and analyzed using repeated-measures ANOVA following square-root transformation.

For determination of the effect of nicotine on both active exploration and under habituated conditions, the total counts for each individual behavior were determined as the number of 5 sec observation "windows" in which a given behavior was evident, summed over the initial 3 × 15 min (0–15, 20–35, and 40–55 min) cycle periods and expressed as means ± SEM. Data for individual behaviors were analyzed using ANOVA following square-root transformation; data were then analyzed using either Student's *t* test or Mann–Whitney *U* test to identify those particular drug doses at which responsivity differed by genotype, for a given topography of behavior.

For determination of rotarod performance, latency to fall was calculated for each mouse on three occasions each day, for 3 successive days, and expressed as means ± SEM. Data were analyzed using ANOVA following square-root transformation; data were then analyzed using either Student's *t* test or Mann–Whitney *U* test to identify those particular time points at which responsivity differed by genotype. For elevated plus-maze performance, the percentage of time spent in and number of entries into open and closed arms was calculated for each mouse. Data were expressed and analyzed as above to identify those particular parameters for which responsivity differed by genotype.

RESULTS

Mice homozygous for the α_4 nAChR mutation were born in the expected mendelian proportion, were capable of reproduction, and were of normal body weight (data not shown). Hematoxylin and eosin-stained sections of the brain of Mt were examined histologically, and no differences in the size or location of the brain nuclei or cortical lamination were apparent (data not shown). In addition, gross anatomical and histological screening failed to show any abnormalities in heart, liver, spleen, kidney, lung, muscle, and thymus (data not shown).

In situ hybridization

In situ hybridization performed on a number of animals (Wt, $n = 9$; Hz, $n = 6$; and Mt, $n = 9$) identified a strong hybridization signal for ISAChα3 and ISAChβ4 localized to the thalamus (Th) and cortex (Cx) in Wt (Fig. 2*E*,*G*) Mt (Fig. 2*F*,*H*), and Hz (data not shown). A moderate hybridization signal was also seen in the caudate putamen (CPu), hippocampus (Hp), dentate gyrus (DG), and substantia nigra (SN) (data not shown). ISAChβ1 and ISAChβ2 probes, which hybridize to the deleted sequence, showed no regional-specific signal throughout the brain of Mt (Fig. 2*B*,*D*) and a reduced signal in Hz (data not shown). The hybridization pattern seen in Wt using ISAChβ1 and ISAChβ2 probes was the same as for ISAChβ3 and ISAChβ4 (Fig. 2*E*,*G*). *In situ* hybridization was also performed for α_3, α_6, α_7, β_2, β_3, and β_4 nAChR subunits (Fig. 3). An intense signal for α_3 mRNA was detected in the medial habenular (MHb) (Fig. 3*A*,*B*), α_6 signal was detected in the SN (Fig. 3*C*,*D*), α_7 was seen in the Hp and DG (Fig. 3*E*,*F*), β_2 showed a strong signal in the MHb and Th, and moderate hybridization was seen in the Cx, Hp, and DG (Fig. 3*G*,*H*), whereas β_3 had limited distribution with signal only in the MHb and the SN (Fig. 3*I*–*L*). β_4 expression was restricted to the MHb (Fig. 3*M*,*N*). There were no statistically significant differences between Mt and Wt in the relative abundance of α_3, α_6, α_7, β_2, β_3, and β_4 nAChR subunits transcripts (Fig. 4). Furthermore, the level of the α_4 nAChR subunit-specific transcripts detected by probes ISAChβ3/4 were the same in Mt and Wt (Fig. 4). These oligonucleotide probes were designed to hybridize to mRNA transcribed from preserved DNA upstream of deleted gene sequence and thereby specifically identify α_4 nAChR subunit-positive cells.

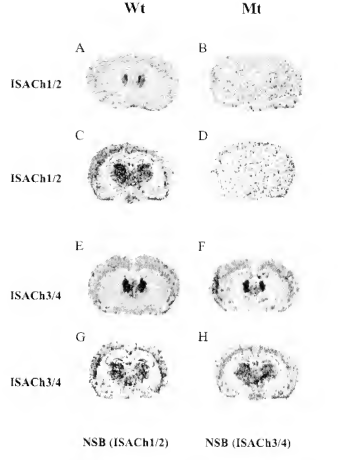

Figure 2. Expression of the α_4 neuronal nAChR subunit in Wt and Mt mouse brain. *In situ* hybridization using antisense α_4 nAChR-specific cDNA oligonucleotide probes. *A*, *C*, *E*, and *G* represent sections from Wt. *B*, *D*, *F*, and *H* were sections derived from Mt. *I* and *J* represent nonspecific binding (*NSB*). Sections shown in *A–D* were probed simultaneously with probes ISAChβ1 and ISAChβ2, whereas sections shown in *E–H* were probed with ISAChβ3 and ISAChβ4. No anatomically defined signal was seen in the Mt with ISAChβ1/ISAChβ2, which detects the deleted sequence (*B*, *D*), whereas signal was detected (in brain regions known to express α_4 nAChR) using ISAChβ3/ISAChβ4, which recognizes upstream transcript (*F*, *H*). Sections shown in *A*, *B*, *E*, and *F* are taken at bregma levels −0.8, and *C*, *D*, *G*, and *H* are taken at bregma levels −1.82 (Franklin and Paxinos, 1997).

Receptor autoradiography

Autoradiographic ligand binding experiments were performed on a number of animals (Wt, $n = 9$; Hz, $n = 11$; and Mt, $n = 11$). Binding experiments conducted in Wt using tritiated nicotine, cytisine, and epibatidine showed a similar pattern of high-affinity binding (Fig. 5). [^{3}H]nicotine labeling was detected at highest levels in the thalamic nuclei, MHb, interpeduncular nucleus (IPn),

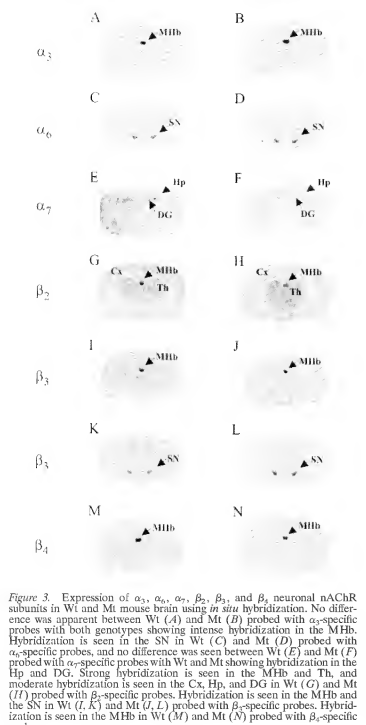

Figure 3. Expression of α_3, α_6, α_7, β_2, β_3, and β_4 neuronal nAChR subunits in Wt and Mt mouse brain using *in situ* hybridization. No difference was apparent between Wt (*A*) and Mt (*B*) probed with α_3-specific probes with both genotypes showing intense hybridization in the MHb. Hybridization is seen in the SN in Wt (*C*) and Mt (*D*) probed with α_6-specific probes, and no difference was seen between Wt (*E*) and Mt (*F*) probed with α_7-specific probes with Wt and Mt showing hybridization in the Hp and DG. Strong hybridization is seen in the MHb and Th, and moderate hybridization is seen in the Cx, Hp, and DG in Wt (*G*) and Mt (*H*) probed with β_2-specific probes. Hybridization is seen in the MHb and the SN in Wt (*I*, *K*) and Mt (*J*, *L*) probed with β_3-specific probes. Hybridization is seen in the MHb in Wt (*M*) and Mt (*N*) probed with β_4-specific probes.

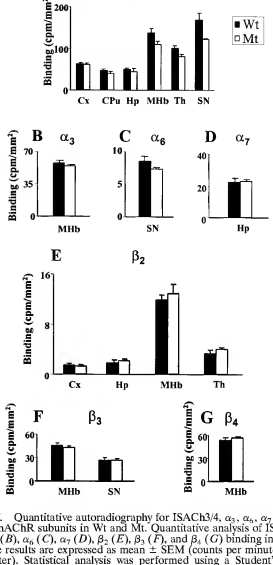

Figure 4. Quantitative autoradiography for ISACh3/4, α_3, α_6, α_7, β_2, β_3, and β_4 nAChR subunits in Wt and Mt. Quantitative analysis of ISACh3/4 (*A*), α_3 (*B*), α_6 (*C*), α_7 (*D*), β_2 (*E*), β_3 (*F*), and β_4 (*G*) binding in Wt and Mt. The results are expressed as mean ± SEM (counts per minute/square millimeter). Statistical analysis was performed using a Student's *t* test. There were no statistically significant differences between Mt and Wt for any of the probes examined. Regions quantitated were Cx, CPu, Th, MHb, SN, and Hp.

superior colliculus (SC), and presubiculum, and moderate levels were found in the Cx, CPu, and fasciculus retroflexus (fr) (Fig. 5*A*,*E*,*I*). [^{3}H]eytisine (Fig. 5*M*) binding showed a similar pattern to [^{3}H]nicotine binding in Wt. [^{3}H]epibatidine (Fig. 5*C*,*G*,*K*) binding differed from [^{3}H]nicotine binding in that [^{3}H]epibatidine binding to the MHb and fr was more intense as shown by quantitative analysis (Fig. 6). [^{3}H]nicotine and [^{3}H]epibatidine binding showed a qualitatively similar pattern in Mt, with binding for both radioligands detected in the MHb, IPn, fr, and SC (Fig. 5). The main difference was that [^{3}H]epibatidine binding was detected at high levels in MHb, IPn, fr, and SC (Fig. 5*D*,*H*,*L*). [^{3}H]eytisine binding was only detected in the IPn of Mt (Fig. 5*N*). [^{3}H]epibatidine binding in Wt and Mt with eytisine or nicotine cold competition resulted in loss of SC signal but preservation of binding in the habenulo-interpeduncular pathway (i.e., MHb, IPn, and fr) (data not shown). [^{125}I]α-bungarotoxin binding was found to be unchanged in Mt compared with Wt (Fig. 5*O*,*P*). Autoradiographic ligand binding experiments performed on an independently generated line of α_4 nAChR subunit knock-out mice (Marubio et al., 1999) also demonstrated high level binding to [^{3}H]epibatidine in a number of nuclei and reduced [^{3}H]nicotine binding in the MHb. Quantitative autoradiography, however, demonstrated that [^{3}H]epibatidine binding was reduced in Mt compared with Wt in the SC and IPn, whereas there was no difference in the MHb (Fig. 6). Furthermore, Marubio et al. (1999) showed that [^{3}H]nicotine binding was found at reduced levels only in the MHb, whereas we detected [^{3}H]nicotine binding in both the IPn and the SC, in addition to the previously described binding sites in the MHb (Fig. 6). Quantitative analysis confirmed that [^{3}H]nicotine binding was moderately reduced in Mt compared with Wt in all three nuclei (Fig. 6).

Topography of spontaneous behavior

General observation

No gross neurological deficits were apparent in 40 Mt (20 females, weight of 25.97 ± 0.53 gm; 20 males, weight of 31.79 ± 0.87 gm; age

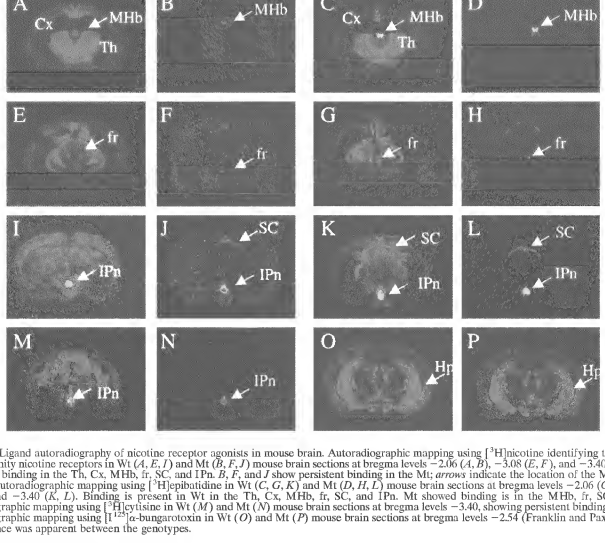

Figure 5. Ligand autoradiography of nicotine receptor agonists in mouse brain. Autoradiographic mapping using [^{3}H]nicotine identifying the presence of high-affinity nicotine receptors in Wt (*A*, *E*, *I*) and Mt (*B*, *F*, *J*) mouse brain sections at bregma levels −2.06 (*A*, *B*), −3.08 (*E*, *F*), and −3.40 (*I*, *J*). *A*, *E*, and *I* show binding in the Th, Cx, MHb, fr, SC, and IPn. *B*, *F*, and *J* show persistent binding in the Mt; *arrows* indicate the location of the MHb, fr, SC, and IPn. Autoradiographic mapping using [^{3}H]epibatidine in Wt (*C*, *G*, *K*) and Mt (*D*, *H*, *L*) mouse brain sections at bregma levels −2.06 (*C*, *D*), −3.08 (*G*, *H*), and −3.40 (*K*, *L*). Binding is present in Wt in the Th, Cx, MHb, fr, SC, and IPn. Mt showed binding is in the MHb, fr, SC, and IPn. Autoradiographic mapping using [^{3}H]cytisine in Wt (*M*) and Mt (*N*) mouse brain sections at bregma levels −3.40, showing persistent binding in the IPn. Autoradiographic mapping using [^{125}I]α-bungarotoxin in Wt (*O*) and Mt (*P*) mouse brain sections at bregma levels −2.54 (Franklin and Paxinos, 1997). No difference was apparent between the genotypes.

of 105 ± 4 d) when compared with 40 Wt controls (20 females, weight of 24.59 ± 59; 20 males, weight of 33.40 ± 0.64 gm; age of 109 ± 6 d); in particular, no epileptic seizures were observed over prolonged observation.

Exploratory phase

Over an initial 1 hr phase of exploratory activity (Fig. 7*A*), Mt were characterized by increased sniffing (+13%; $F_{(1,76)} = 6.76$, $p = 0.01$) and decreased grooming (−15%; $F_{(1,76)} = 4.98$, $p = 0.03$), for both genders; females groomed less than males for each genotype.

Habituation phase

Over the subsequent phase of habituation (Fig. 7*B*), additional effects were evident. Each of sniffing, total rearing, rearing seated, rearing to wall, rearing free, and chewing occurred to excess in Mt throughout this phase ($F_{(1,76)} = 17.56$, $p < 0.001$; $F_{(1,76)} = 14.95$, $p < 0.001$; $F_{(1,76)} = 13.96$, $p < 0.001$; $F_{(1,76)} = 16.15$, $p < 0.001$; $F_{(1,76)} = 4.94$, $p < 0.05$; $F_{(1,76)} = 5.19$, $p < 0.05$, respectively); for those behaviors that declined significantly by time bins (i.e., habituation of sniffing, total rearing, rearing seated, and rearing to wall), this did not differ by genotype or gender, whereas for those low-frequency behaviors for which habituation was not apparent (i.e., rearing free and chewing), males habituated more rapidly than did females for each genotype. Locomotion also occurred to excess in Mt ($F_{(1,76)} = 11.11$, $p = 0.001$) because of their reduced rate of habituation (time × genotype interaction, $F_{(10,760)} = 1.97$, $p = 0.03$) for both genders. Although overall levels of grooming were comparable, this behavior varied over time bins in a manner that differed between the genotypes (time × genotype interaction, $F_{(10,760)} = 3.38$, $p < 0.001$) for both genders. Overall levels of stillness were decreased in Mt ($F_{(1,76)} = 24.83$, $p < 0.001$) because of their reduced rate of habituation (time × genotype interaction, $F_{(10,760)} = 1.98$, $p = 0.03$) for both genders.

In summary, over an initial exploratory phase, Mt showed increased sniffing with decreased grooming. Over the subsequent habituation phase, increased sniffing in Mt endured together with the emergence of increases in most other topographies of behavior; in particular, increased locomotion in Mt was characterized by a reduced rate of habituation relative to Wt.

Rotarod performance

Among 37 Mt (15 females, weight of 25.01 ± 0.58; 22 males, weight of 31.32 ± 0.8 gm; age of 97 ± 3 d) and 44 Wt controls (20 females, weight of 24.45 ± 0.76; 24 male, weight of 33.27 ± 0.51 gm; age of 96 ± 5 d), performance improved with time (three trials on each of 3 successive test days, $F_{(8,632)} = 18.47$, $p < 0.001$) in a manner that did not differ by genotype or gender (Fig. 8). Thus, in this test of sensorimotor coordination, Mt evidenced no deficits.

Elevated plus-maze performance

When compared with 51 Wt controls (21 females, weight of 24.2 ± 0.47; 30 males, weight of 31.44 ± 1.0 gm; age of 96 ± 5 d), 70 Mt (36 females, weight of 25.7. ± 0.47; 34 males, weight of 32.81 ± 0.71 gm; age of 97 ± 3 d) spent less time in open arms ($F_{(1,115)} = 6.92$, $p < 0.01$) and made fewer open-arm entries ($F_{(1,115)} = 6.9$, $p < 0.01$) in a manner that did not differ by gender (Fig. 9); for each

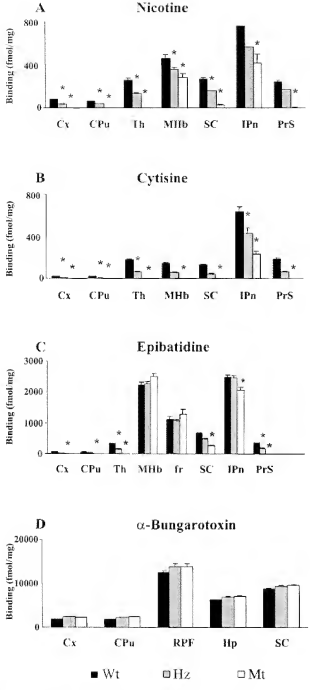

Figure 6. Quantitative autoradiography for nicotinic agonists in the mouse brain. Quantitative analysis of [^{3}H]nicotine (*A*), [^{3}H]cytisine (*B*), [^{3}H]epibatidine (*C*), and [^{125}I]α-bungarotoxin (*D*) binding in Wt, Hz, and Mt. The results are expressed as mean ± SEM (femtomoles per milligram). Statistical analysis was performed using a one-way ANOVA. *$p < 0.05$ versus Wt controls. Regions quantitated were Cx, CPu, Th, MHb, SC, IPn, fr, retroparafasciculus (*RPF*), and Hp. *PrS*, Presubiculum.

genotype, males entered fewer arms than females. Thus, in this test of "anxiety-like" behavior, Mt evidenced heightened levels.

Effects of nicotine: unhabituated condition

Our results differed from those of Marubio et al. (1999), who analyzed an independently generated line of α_4 nAChR subunit knock-out mice, finding no significant differences from baseline in nonhabituated locomotor activity in response to 1 or 2 mg/kg nicotine. When comparing 40 Mt (20 females, weight of 25.62 ± 0.46; 20 males, weight of 31.55 ± 0.82 gm; age of 97 ± 3 d) with 40 Wt controls (20 females, weight of 25.16 ± 0.45; 20 males, weight of 32.47 ± 0.55 gm; age 100 ± 2 d), declines in each of sniffing, locomotion, and total rearing over the three time periods were influenced by dose of nicotine administered in a genotype-specific manner (genotype × dose × time interactions, $F_{(8,120)} = 2.23$, $p = 0.03$; $F_{(8,120)} = 3.98$, $p < 0.001$; $F_{(8,120)} = 2.16$, $p < 0.05$, respectively) (Fig. 10*A–C*). For sifting, a generally comparable although blunted profile was apparent (Fig. 10*D*). For individual topographies of rearing, grooming, and chewing, less consistent profiles of effect were apparent (data not shown).

In summary, under this unhabituated condition, Mt showed less decline in sniffing, locomotion, total rearing, and sifting over these three time periods than was evident in Wt; decline in behavior in Mt was restored by low to mid doses of nicotine, particularly over the late (40–55 min) period.

Effects of nicotine: habituated condition

When comparing 20 Mt (10 females, weight of 25.2 ± 0.7; 10 males, weight of 33.2 ± 0.2 gm; age of 95 ± 3 d) with 20 Wt controls (10 females, weight of 26.28 ± 0.6; 10 males, weight of 32.38 ± 0.38 gm; age of 95 ± 5 d), each of sniffing, locomotion, and total rearing declined over the three time periods; for locomotion and total rearing, an action of nicotine to reduce these behaviors declined with time in a manner that was influenced by dose of nicotine administered (dose × time interactions, $F_{(8,120)} = 3.14$, $p = 0.01$; $F_{(8,120)} = 4.64$, $p < 0.001$, respectively) (Fig. 11*A–C*). For sifting, a generally comparable although blunted profile was apparent (Fig. 11*D*), and for individual topographies of rearing, grooming, and chewing, similar profiles of effect were apparent (data not shown).

In summary, under this habituated condition, lower levels of behavior continued to decline with time; nicotine acted mainly to further reduce behavior, primarily over the early (20–35 min) period, in a manner that tended to be less prominent in Mt than in Wt. Thus, the above late-period action of nicotine to restore in Mt a Wt-like behavioral profile appeared specific to the unhabituated condition.

DISCUSSION

The $\alpha_4\beta_2$ subunit receptor configuration, known to be expressed at high levels in the thalamus and the habenulo-interpeduncular system (Zoli et al., 1998), is responsible for the vast majority of agonist binding. In this study, we have characterized the binding patterns of a number of nicotinic agonists in normal and α_4 nAChR knock-out mice. These data combined with the results of previous studies (Zoli et al., 1998) on mice lacking functional β_2 nAChRs allows us to further characterize brain nAChRs. Mt maintain high-level [^{3}H]nicotine binding in the MHb and IPn and low-level binding in the SC and fr, whereas the β_2 knock-out mice showed no binding with this ligand (Picciotto et al., 1995). β_2 knock-out mice had [^{3}H]cytisine binding sites in the MHb, IPn, and fr (Zoli et al., 1998), whereas Mt had binding in the IPn but not in the MHb or fr. β_2 knock-out mice differ from Mt in that Mt showed additional [^{3}H]epibatidine binding sites in the SC. Our [^{3}H]nicotine autoradiography results differed from ligand binding experiments performed on an independently generated line of α_4 nAChR knock-out mice (Marubio et al., 1999). In this earlier study, [^{3}H]nicotine binding was found at low levels only in the MHb, whereas we detected additional low-level binding sites in the IPn, SC, and fr (Figs. 5, 6).

There are known to be high levels of α_3 and α_4 (Wada et al., 1989) and low levels of α_6 mRNA (Le Novere et al., 1996) in the rodent MHb, whereas all β subunits surveyed are detected in this nucleus (Deneris et al., 1989; Duvoisin et al., 1989; Wada et al., 1989). We found no significant differences in the expression profile of a large number of subunits within the MHb of Mt and Wt. A strong hybridization signal was detected for α_3, β_2, β_3, and β_4, confirming the results of previous studies (Le Novere et al., 1996). The receptor configuration responsible for the MHb binding to [^{3}H]nicotine seen in Mt therefore involves the β_2 subunit in combination with the α_3 subunit expressed at high levels and/or the α_6 subunit expressed at low levels. Nicotine autoradiographic analysis

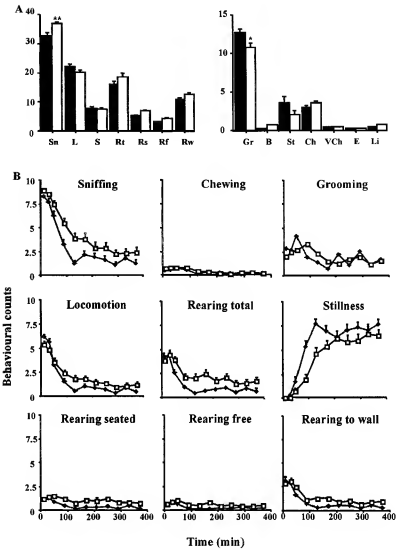

Figure 7. *A*, Behavioral counts for sniffing (*Sn*), locomotion (*L*), sifting (*S*), total rearing (*Rt*), rearing from a seated position (*Rs*), rearing free (*Rf*), rearing to wall (*Rw*), grooming (*Gr*), biting (*B*), stillness (*St*), chewing (*Ch*), vacuous chewing (*VCh*), eating (*E*), and licking (*Li*) in Wt ($n = 40$; *filled columns*) versus Mt ($n = 40$; *open columns*). Data are mean ± SEM counts over a 1 hr phase of initial exploratory activity. $^{***}p < 0.001$, $^{**}p < 0.01$, $^{*}p < 0.05$ versus wild-types. *B*, Behavioral counts for sniffing, eating, grooming, locomotion, rearing total, stillness, rearing seated, rearing free, and rearing to wall in Wt ($n = 40$; *squares*) versus Mt ($n = 40$; *diamonds*). Data are mean ± SEM counts per 10 min period at indicated intervals over habituation phase.

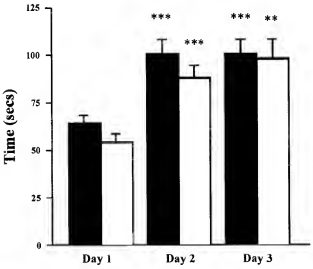

Figure 8. Performance on a repeated motor coordination task in Wt ($n = 37$; *filled columns*) versus Mt ($n = 44$; *open columns*). Mice were evaluated on the rotarod test three times a day for 3 consecutive days. Data are presented as the mean ± SEM of the daily averages. $^{***}p < 0.001$, $^{**}p < 0.01$ versus same genotype on day 1.

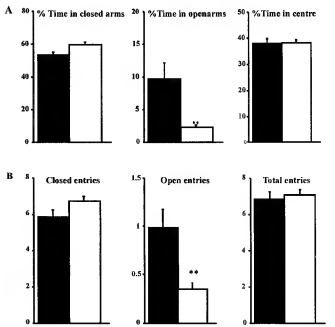

Figure 9. The elevated plus-maze assay. Data are presented as the mean ± SEM of percentage time in (*A*) and number of entries into (*B*) various sectors in Wt ($n = 51$; *filled columns*) and Mt ($n = 70$; *open columns*). $^{**}p < 0.01$, $^{*}p < 0.05$ versus Wt.

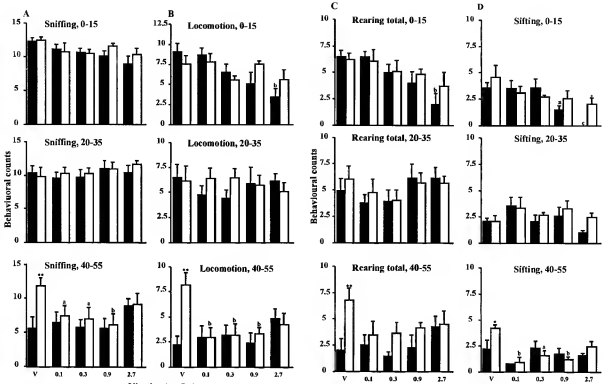

Figure 10. Unhabituated mice: response to nicotine administration. Behavioral counts summed over 0–15, 20–35, and 40–55 min: sniffing (*A*), locomotion (*B*), rearing total (*C*), and sifting (*D*) responses to (−)-nicotine (0.1–2.7 mg/kg, s.c.) versus vehicle (*V*) in unhabituated Wt (*filled* columns) and Mt (*open columns*). Data are means ± SEM for $n = 8$ per group. $^{**}p < 0.01$, $^{*}p < 0.05$ versus Wt. $^{a}p < 0.05$, $^{b}p < 0.01$, $^{c}p < 0.001$ versus vehicle-treated mice of same genotype.

in β_2 knock-out mice suggests that the β_3 and β_4 expression detected in the MHb is insufficient to mediate [^{3}H]nicotine binding. The finding that β_2 knock-out mice retain high-affinity [^{3}H]cytisine binding in the MHb and that Mt lack MHb binding confirms that cytisine binding in the MHb requires the α_4 subunit but does not require the β_2 subunit. [^{3}H]epibatidine binding was detected in the MHb of both knock-out lines, suggesting that [^{3}H]epibatidine binding can occur in the absence of β_2 or α_4 subunits.

A detailed, topographical analysis of spontaneous and nicotine-stimulated behavior was undertaken. Over the initial 1 hr exploratory phase, Mt showed an increase in sniffing and a reduction in grooming. Over the subsequent phase of habituation, additional effects were revealed as certain topographies of behavior did not habituate to the same extent in Mt. For sniffing, both genotypes habituated to similar extents, whereas for locomotion and topographies of rearing and chewing, Mt retained a higher level of activity throughout the habituation phase. Alterations in "motor activity" after nicotine administration have been described previously. Although these studies have most commonly used techniques that fail to resolve individual topographies of behavior (Morrison and Stephenson, 1972; Clarke and Kumar, 1983; Clarke, 1987), state-dependency of effect, e.g., treatment in a familiar versus novel environment, has been reported (Picciotto et al., 2000). Using the present ethologically based approach, over the first 15 min of the exploratory phase, nicotine induced in Wt a dose-dependent reduction in locomotion, total rearing, sifting, and less so in sniffing, although there was no such drug effect in Mt; rather, as above, Mt showed relative preservation of these behaviors over the exploratory phase, with late decline in behavior restored in Mt to Wt levels by low to mid doses of nicotine. Under the habituated condition, however, during which lower levels of behavior continued to decline with time, nicotine was still able to further reduce locomotion, total rearing, sifting, and less so in sniffing; this occurred primarily over the early period in a manner that tended to be less prominent in Mt than in Wt. Thus, the above late-period action of nicotine to restore in Mt a Wt-like behavioral profile appeared specific to the unhabituated condition. The lack of modulation of locomotion and sniffing behavior in Mt with high doses of nicotine (Fig. 10) may reflect pharmacological desensitization of remaining nicotinic receptors (Couturier et al., 1990; Vibat et al., 1995; Fenster et al., 1997). These data indicate a topographically specific interaction between α_4 nAChR knock-out and the neuronal processes of habituation in determining not only the regulation of spontaneous behavior but also the effects of nicotine on behavior.

One hypothesis is that the α_4 nAChR subunit is required for activation of inhibitory neural circuits; hence, its absence would result in an elevated baseline of specific behavioral topographies. Pharmacological doses of nicotine may nonetheless act through non-α_4 nAChR-containing nicotine binding sites, perhaps those present in the habenulo-interpeduncular pathway, to reduce inhibitory tone. However, this might only be evident when such inhibitory neural tone is at a low level, as would be expected in actively exploring mice; the delayed effect of nicotine administration in reducing locomotion, sniffing, rearing, and sifting in this exploratory condition may reflect some temporal inefficiency of this parallel pathway in responding to change. Furthermore, the effect of an agent that acts primarily to activate inhibitory pathways may be less apparent in well habituated mice in which inhibitory pathways (both nAChR-dependent and -independent) might be already prominently activated. There are a number of studies describing nicotine-induced release of the inhibitory neurotransmitter GABA either from isolated synaptosomes or in slice preparations (Lena et al., 1993; Kayadjanian et al., 1994; McMahon et al., 1994). Of particular relevance to our findings is the observation of Lena et al. (1993) showing that nicotine increases the frequency of postsynaptic GABAergic currents in rat interpeduncular nucleus neurons.

Nicotinic receptor agonists that bind the α_4/β_2 receptor config-

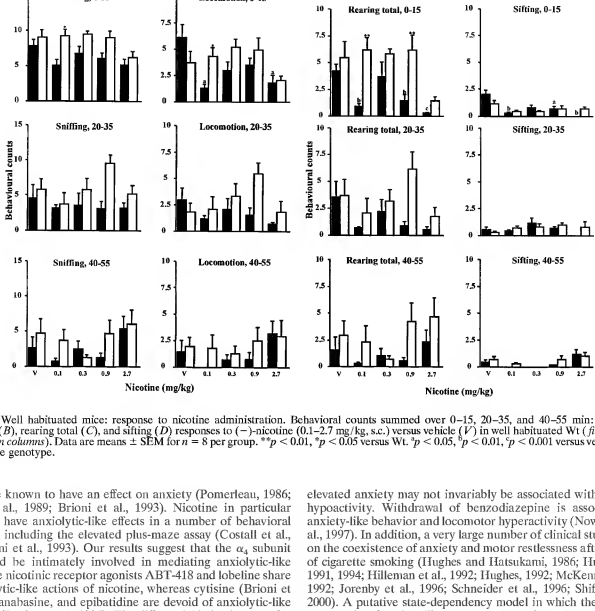

Figure 11. Well habituated mice: response to nicotine administration. Behavioral counts summed over 0–15, 20–35, and 40–55 min: sniffing (*A*), locomotion (*B*), rearing total (*C*), and sifting (*D*) responses to (−)-nicotine (0.1–2.7 mg/kg, s.c.) versus vehicle (*V*) in well habituated Wt (*filled columns*) and Hz (*open columns*). Data are means ± SEM for $n = 8$ per group. $^{**}p < 0.01$, $^{*}p < 0.05$ versus Wt. $^{a}p < 0.05$, $^{b}p < 0.01$, $^{c}p < 0.001$ versus vehicle-treated mice of same genotype.

uration are known to have an effect on anxiety (Pomerleau, 1986; Gilbert et al., 1989; Brioni et al., 1993). Nicotine in particular appears to have anxiolytic-like effects in a number of behavioral paradigms, including the elevated plus-maze assay (Costall et al., 1989; Brioni et al., 1993). Our results suggest that the α_4 subunit may indeed be intimately involved in mediating anxiolytic-like effects. The nicotinic receptor agonists ABT-418 and lobeline share the anxiolytic-like actions of nicotine, whereas cytisine (Brioni et al., 1993), anabasine, and epibatidine are devoid of anxiolytic-like properties (Decker et al., 1995). The differential behavioral profile of neuronal nicotinic agonists implies that the anxiolytic-like actions may be mediated by a specific subunit configuration of the nAChR. If this were indeed the case, we would expect agonists that have similar effects on anxiety to have comparable ligand binding profiles with respect to both qualitative (i.e., topography of binding) and quantitative (i.e., agonist specific intensity of binding) parameters. The differential preservation of binding in Mt may explain the lack of anxiolytic-like effects seen with cytisine because it implies selectivity for a specific receptor subpopulation, but it would not readily explain the lack of anxiolytic-like effect of epibatidine because the binding pattern of epibatidine is qualitatively similar to nicotine in Mt. Quantitative autoradiographic analysis demonstrates comparable epibatidine binding in Wt and Mt in the MHb and fr (although a minor reduction of epibatidine binding of 16% in the IPn of Mt compared with Wt). In contrast, nicotine binding shows a substantial reduction of 40% in the MHb and 45% in the IPn in Mt compared with Wt. The situation is further complicated by the potential for differential segregation of nAChR subunits on individual neurons.

The finding of increased exploratory activity evident on assessment of spontaneous behavior was surprising given the anxiety-like profile demonstrated by elevated plus-maze analysis. However, elevated anxiety may not invariably be associated with locomotor hypoactivity. Withdrawal of benzodiazepine is associated with anxiety-like behavior and locomotor hyperactivity (Nowakowska et al., 1997). In addition, a very large number of clinical studies report on the coexistence of anxiety and motor restlessness after cessation of cigarette smoking (Hughes and Hatsukami, 1986; Hughes et al., 1991, 1994; Hilleman et al., 1992; Hughes, 1992; McKenna and Cox, 1992; Jorenby et al., 1996; Schneider et al., 1996; Shiffman et al., 2000). A putative state-dependency model in which the behavioral topography of anxiety-like responses depends on the environmental context may be useful in understanding the data. In this model, the sustained level of behavior in mutants over habituation in a "naturalistic" setting would appear to compliment the finding of reduced open-arm entries in the "stressful" setting of the plus-maze.

In conclusion, our data suggests that, in a stressful setting, Mt have a heightened basal level of anxiety-like behavior; furthermore, in a naturalistic setting, topographies of exploratory behavior are increased, and these behaviors may nonetheless be modulated by nicotine administration.

REFERENCES

Brioni JD, O'Neill AB, Kim DJ, Decker MW (1993) Nicotinic receptor agonists exhibit anxiolytic-like effects on the elevated plus-maze test. Eur J Pharmacol 238:1–8.

Brioni JD, Decker MW, Sullivan JP, Arneric SP (1997) The pharmacology of (−)-nicotine and novel cholinergic channel modulators. Adv Pharmacol 37:153–214.

Cao W, Burkholder T, Wilkins L, Collins AC (1993) A genetic comparison of behavioral actions of ethanol and nicotine in the mirrored chamber. Pharmacol Biochem Behav 45:803–809.

Changeux JP, Bertrand D, Corringer PJ, Dehaene S, Edelstein S, Lena C, Le Novere N, Marubio L, Picciotto M, Zoli M (1998) Brain nicotinic receptors: structure and regulation, role in learning and reinforcement. Brain Res Brain Res Rev 26:198–216.

Clarke PB (1987) Nicotine and smoking: a perspective from animal studies. Psychopharmacology 92:135–143.
Clarke PB, Kumar R (1983) The effects of nicotine on locomotor activity in non-tolerant and tolerant rats. Br J Pharmacol 78:329–337.
Clifford JJ, Waddington JL (1998) Heterogeneity of behavioural profile between three new putative selective D3 dopamine receptor antagonists using an ethologically based approach. Psychopharmacology (Berl) 136:284–290.
Clifford JJ, Tighe O, Croke DT, Sibley DR, Drago J, Waddington JL (1998) Topographical evaluation of the phenotype of spontaneous behaviour in mice with targeted gene deletion of the $D1_A$ dopamine receptor: paradoxical elevation of grooming syntax. Neuropharmacology 37:1595–1602.
Clifford JJ, Tighe O, Croke DT, Kinsella A, Sibley DR, Drago J, Waddington JL (1999) Conservation of behavioural topography to dopamine D1-like receptor agonists in mutant mice lacking the D1A receptor implicates a D1-like receptor not coupled to adenylyl cyclase. Neuroscience 93:1483–1489.
Corringer PJ, Galzi JL, Eisele JL, Bertrand S, Changeux JP, Bertrand D (1995) Identification of a new component of the agonist binding site of the nicotinic alpha 7 homooligomeric receptor. J Biol Chem 270:11749–11752.
Costall B, Kelly ME, Naylor RJ, Onaivi ES (1989) The actions of nicotine and cocaine in a mouse model of anxiety. Pharmacol Biochem Behav 33:197–203.
Court J, Perry E (1995) Distribution of nicotinic receptors in the CNS In: CNS neurotransmitters and neuromodulators: acetylcholine (Stone TW, ed), pp 85–104. Boca Raton, FL: CRC.
Couturier S, Bertrand D, Matter JM, Hernandez MC, Bertrand S, Millar N, Valera S, Barkas T, Ballivet M (1990) A neuronal nicotinic acetylcholine receptor subunit (alpha 7) is developmentally regulated and forms a homo-oligomeric channel blocked by alpha-BTX. Neuron 5:847–856.
Damaj MI, Fei-Yin M, Dukat M, Glassco W, Glennon RA, Martin BR (1998) Antinociceptive responses to nicotinic acetylcholine receptor ligands after systemic and intrathecal administration in mice. J Pharmacol Exp Ther 284:1058–1065.
Decker MW, Brioni JD, Bannon AW, Arneric SP (1995) Diversity of neuronal nicotinic acetylcholine receptors: lessons from behavior and implications for CNS therapeutics. Life Sci 56:545–570.
Deneris ES, Boulter J, Swanson LW, Patrick J, Heinemann S (1989) Beta 3: a new member of nicotinic acetylcholine receptor gene family is expressed in brain. J Biol Chem 264:6268–6272.
Drago J, Gerfen CR, Lachowicz JE, Steiner H, Hollon TR, Love PE, Ooi GT, Grinberg A, Lee EJ, Huang SP, Bartlet PF, Jose PA, Sibley DR, Westphal H (1994) Altered striatal function in a mutant mouse lacking D1A dopamine receptors. Proc Natl Acad Sci USA 91:12564–12568.
Duvoisin RM, Deneris ES, Patrick J, Heinemann S (1989) The functional diversity of the neuronal nicotinic acetylcholine receptors is increased by a novel subunit: beta 4. Neuron 3:487–496.
Elgoyhen AB, Johnson DS, Boulter J, Vetter DE, Heinemann S (1994) Alpha 9: an acetylcholine receptor with novel pharmacological properties expressed in rat cochlear hair cells. Cell 79:705–715.
Fenster CP, Rains MF, Noerager B, Quick MW, Lester RA (1997) Influence of subunit composition on desensitization of neuronal acetylcholine receptors at low concentrations of nicotine. J Neurosci 17:5747–5759.
Franklin KBJ, Paxinos G (1997) The mouse brain in stereotaxic coordinates. San Diego: Academic.
Giacobini E (1991) Nicotinic cholinergic receptors in human brain: effects of aging and Alzheimer. Adv Exp Med Biol 296:303–315.
Gilbert DG (1979) Paradoxical tranquilizing and emotion-reducing effects of nicotine. Psychol Bull 86:643–661.
Gilbert DG, Robinson JH, Chamberlin CL, Spielberger CD (1989) Effects of smoking/nicotine on anxiety, heart rate, and lateralization of EEG during a stressful movie. Psychophysiology 26:311–320.
Hill JR JA, Zoli M, Bourgeois JP, Changeux JP (1993) Immunocytochemical localization of a neuronal nicotinic receptor: the beta 2-subunit. J Neurosci 13:1551–1568.
Hilleman DE, Mohiuddin SM, Del Core MG, Sketch Sr MH (1992) Effect of buspirone on withdrawal symptoms associated with smoking cessation. Arch Intern Med 152:350–352.
Hughes JR (1992) Tobacco withdrawal in self-quitters. J Consult Clin Psychol 60:689–697.
Hughes JR, Hatsukami D (1986) Signs and symptoms of tobacco withdrawal. Arch Gen Psychiatry 43:289–294.
Hughes JR, Gust SW, Skoog K, Keenan RM, Fenwick JW (1991) Symptoms of tobacco withdrawal. A replication and extension. Arch Gen Psychiatry 48:52–59.
Hughes JR, Higgins ST, Bickel WK (1994) Nicotine withdrawal versus other drug withdrawal syndromes: similarities and dissimilarities. Addiction 89:1461–1470.
Hutchinson RR, Emley GS (1973) In: Smoking behavior: motives and incentives (Dunn WL, ed), pp 171–196. Washington DC: Winston and Sons.
Jorenby DE, Hatsukami DK, Smith SS, Fiore MC, Allen S, Jensen J, Baker TB (1996) Characterization of tobacco withdrawal symptoms: transdermal nicotine reduces hunger and weight gain. Psychopharmacology (Berl) 128:130–138.
Kayadjanian N, Retaux S, Menetrey A, Besson MJ (1994) Stimulation by nicotine of the spontaneous release of [^{3}H]gamma-aminobutyric acid in the substantia nigra and in the globus pallidus of the rat. Brain Res 649:129–135.
Le Novere N, Changeux JP (1995) Molecular evolution of the nicotinic acetylcholine receptor: an example of multigene family in excitable cells. J Mol Evol 40:155–172.
Le Novere N, Zoli M, Changeux JP (1996) Neuronal nicotinic receptor alpha 6 subunit mRNA is selectively concentrated in catecholaminergic nuclei of the rat brain. Eur J Neurosci 8:2428–2439.
Lena C, Changeux JP, Mulle C (1993) Evidence for "preterminal" nicotinic receptors on GABAergic axons in the rat interpeduncular nucleus. J Neurosci 13:2680–2688.
Marubio LM, del Mar Arroyo-Jimenez M, Cordero-Erausquin M, Lena C, Le Novere N, de Kerchove d'Exaerde A, Huchet M, Damaj MI, Changeux JP (1999) Reduced antinociceptive effects in mice lacking neuronal nicotinic receptor subunits. Nature 398:805–810.
McKenna JP, Cox JL (1992) Transdermal nicotine replacement and smoking cessation. Am Fam Physician 45:2595–2602.
McMahon LL, Yoon KW, Chiappinelli VA (1994) Nicotinic receptor activation facilitates GABAergic neurotransmission in the avian lateral spiriform nucleus. Neuroscience 59:689–698.
Morrison CF, Stephenson JA (1972) The occurrence of tolerance to a central depressant effect of nicotine. Br J Pharmacol 46:151–156.
Nowakowska E, Chodera A, Kus K (1997) Pharmacological aspects of withdrawal from certain benzodiazepines. Pol J Pharmacol 49:89–95.
Orr-Urtreger A, Goldner FM, Saeki M, Lorenzo I, Goldberg L, De Biasi M, Dani JA, Patrick JW, Beaudet AL (1997) Mice deficient in the alpha7 neuronal nicotinic acetylcholine receptor lack alpha-bungarotoxin binding sites and hippocampal fast nicotinic currents. J Neurosci 17:9165–9171.
Pellow S, Chopin P, File SE, Briley M (1985) Validation of open:closed arm entries in an elevated plus-maze as a measure of anxiety in the rat. J Neurosci Methods 14:149–167.
Picciotto MR, Zoli M, Lena C, Bessis A, Lallemand Y, LeNovere N, Vincent P, Pich EM, Brulet P, Changeux JP (1995) Abnormal avoidance learning in mice lacking functional high-affinity nicotine receptor in the brain. Nature 374:65–67.
Picciotto MR, Caldarone BJ, King SL, Zachariou V (2000) Nicotinic receptors in the brain. Links between molecular biology and behavior. Neuropsychopharmacology 22:451–465.
Pomerleau OF (1986) Nicotine as a psychoactive drug: anxiety and pain reduction. Psychopharmacol Bull 22:865–869.
Schneider NG, Olmstead RE, Steinberg C, Sloan K, Dains RM, Brown HV (1996) Efficacy of bupirone in smoking cessation: a placebo-controlled trial. Clin Pharmacol Ther 60:568–575.
Shiffman S, Johnston JA, Khayrallah M, Elash CA, Gwaltney CJ, Paty JA, Gnys M, Evoniuk G, DeVeaugh-Geiss J (2000) The effect of bupropion on nicotine craving and withdrawal. Psychopharmacology (Berl) 148:33–40.
Steinlein OK, Mulley JC, Propping P, Wallace RH, Phillips HA, Sutherland GR, Scheffer IE, Berkovic SF (1995) A missense mutation in the neuronal nicotinic acetylcholine receptor alpha 4 subunit is associated with autosomal dominant nocturnal frontal lobe epilepsy. Nat Genet 11:201–203.
Steinlein OK, Magnusson A, Stoodt J, Bertrand S, Weiland S, Berkovic SF, Nakken KO, Propping P, Bertrand D (1997) An insertion mutation of the CHRNA4 gene in a family with autosomal dominant nocturnal frontal lobe epilepsy. Hum Mol Genet 6:943–947.
Tripathi HL, Martin BR, Aceto MD (1982) Nicotine-induced antinociception in rats and mice: correlation with nicotine brain levels. J Pharmacol Exp Ther 221:91–96.
Tybulewicz VL, Crawford CE, Jackson PK, Bronson RT, Mulligan RC (1991) Neonatal lethality and lymphopenia in mice with a homozygous disruption of the c-abl proto-oncogene. Cell 65:1153–1163.
Vibat CR, Lasalde JA, McNamee MG, Ochoa EL (1995) Differential desensitization properties of rat neuronal nicotinic acetylcholine receptor subunit combinations expressed in *Xenopus laevis* oocytes. Cell Mol Neurobiol 15:411–425.
Wada E, Wada K, Boulter J, Deneris E, Heinemann S, Patrick J, Swanson LW (1989) Distribution of alpha 2, alpha 3, alpha 4, and beta 2 neuronal nicotinic receptor subunit mRNAs in the central nervous system: a hybridization histochemical study in the rat. J Comp Neurol 284:314–335.
Wada E, McKinnon D, Heinemann S, Patrick J, Swanson LW (1990) The distribution of mRNA encoded by a new member of the neuronal nicotinic acetylcholine receptor gene family (alpha 5) in the rat central nervous system. Brain Res 526:45–53.
Wong JY, Liberatore GT, Donnan GA, Howells DW (1997) Expression of brain-derived neurotrophic factor and TrkB neurotrophin receptors after striatal injury in the mouse. Exp Neurol 148:83–91.
Xu W, Gelber S, Orr-Urtreger A, Armstrong D, Lewis RA, Ou CN, Patrick J, Role L, De Biasi M, Beaudet AL (1999) Megacystis, mydriasis, and ion channel defect in mice lacking the alpha3 neuronal nicotinic acetylcholine receptor. Proc Natl Acad Sci USA 96:5746–5751.
Zoli M, Lena C, Picciotto MR, Changeux JP (1998) Identification of four classes of brain nicotinic receptors using beta2 mutant mice. J Neurosci 18:4461–4472.